Journal of Corrosion and Materials
www.corromat.com

J. Corros. Mater. **49**(1), 2024 9–23
https://doi.org/10.61336/jcm2024-2

Corrosion Inhibition of Mild Steel With Phenol-Based Anticorrosion Fraction: Preparation, Phytochemistry, and Potentiodynamic Polarization

Yakubu Mary Ohunene[1], Oguegbulu Joseph[1,3], Maia-Obi, Lígia Passos[4], Fanyana faks Mtunzi[5], Francis Ojo[1], Okoli Joseph Bamidele[1,5,*]

[1] *Department of Chemical Sciences, Faculty of Science and Technology, Bingham University, PMB 005, Karu, Nasarawa State, Nigeria.2*
[2] *Department of Chemistry, Nigerian Defence Academy*
[3] *Department of Drug Discovery and Biomedical Sciences, Medical University of South Carolina, 29425, Charleston, South Carolina, USA*
[4] *Center of Engineering, Modeling and Applied Social Sciences (CECS), Federal University of ABC, Brazil.*
[5] *Institute of Chemical and Biotechnology, Vaal University of Technology, Southern Gauteng Science and Technology Park, Private Bag X021, Vanderbijlpark 1911, South Africa.*
(Received: 07 July 2023. Received in revised form: 10 September 2023. Accepted: 20 March 2024. Published online: 30 June 2024.)

Abstract

Corrosion poses a significant threat to various industries, and effective corrosion inhibition strategies are crucial for material integrity and longevity. This study investigates the corrosion inhibition potential of a polyphenol-rich fraction (PRFSS) extracted from the stem bark of *Senegalia senegal*, a drought-tolerant shrub. The PRFSS was evaluated as a green and eco-friendly corrosion inhibitor for mild steel in 1M H_2SO_4 solution. The phytochemical screening of PRFSS revealed the presence of tannins, phenols, and anthocyanins. The potentiodynamic polarization measurement showed that PRFSS significantly inhibited the corrosion of mild steel. The inhibition efficiency increased with increasing PRFSS concentration, suggesting the formation of a protective layer on the metal surface. Thermodynamic studies revealed that the adsorption of PRFSS onto mild steel followed the Langmuir adsorption isotherm, indicating a monolayer coverage. The enthalpy and activation energy of adsorption were negative, suggesting an exothermic and spontaneous adsorption process. The surface characterization using Fourier transform infrared spectroscopy confirmed the adsorption of PRFSS on the metal surface and the formation of a protective film. The study highlights the potential of PRFSS as a sustainable and effective corrosion inhibitor for mild steel in acidic environments. Its eco-friendly nature and biodegradability make it an attractive alternative to conventional corrosion inhibitors, contributing to environmental sustainability. The findings have implications for the development of environmentally benign strategies for corrosion control in various industrial applications.

Keywords: Tannin, Corrosion, Mild steel, Senegalia Senegal, Adsorption studies, thermodynamic studies

1. Introduction

Corrosion is a major threat facing industries and an understanding of preventive measures against corrosion is of high importance. It results in major loss to the integrity of materials, leading to structural failures, injuries, environmental contamination and loss of lives [1]. Mild steel, a fine ferrous metal serves as an important component of tools, equipment, devices and structures used in construction and various industries such as oil and gas, automobiles, medical, chemicals, and aviation [2]. The varied applications of mild steel in industrial processes require contact with acidic corrodent as operation agents, thus facilitating its accelerated corrosion [3]. Some consequences of mild steel corrosion include a reduced availability of industrial parts of economic and technical value, reduced value of aesthetics assets appearance, cost of maintenance and replacement of corroded industrial components, etc [4].

The use of corrosion inhibitors have been reported as a more practical approach to address the challenges of mild steel degradation [5–8]. Corrosion inhibitors are chemical compounds which when added in small concentration to a corrosive environment, form several monomolecular layers which bars steel surfaces from acid attack, thereby decreasing or averting corrosion [9]. They may act as scavengers by weakening the corrodent in the medium or as an interface inhibitor by forming an adsorbed protective film on the mild steel surface pushing it into a passive region and halting the degradation [10].

Corrosion inhibitors that are typically synthesized from organic and inorganic chemicals usually consist of specific chemical moieties such as imidazole, urea, aldehyde, amine, ethyoxylate. Compounds of heavy metals such as lead, cadmium, arsenic, antimony, chromate, tungsten, and molybedum are also used to inhibit corrosion of iron and other metals [11]. Chemically synthesized corrosion inhibitors, however, present the shortcoming of containing heavy metals and unsafe organic moieties, some of which are generally nonbiodegradable, unrecyclable, environmentally unfriendly and toxic with hazardous effects on the ecosystem or simply expensive to synthesize [12]. Growing environmental concerns call for the replacement of chemically synthesized corrosion inhibitors with environmentally benign agents sourced from plants and other natural sources that can inhibit the corrosion of mild steel and other metals [13].

*Corresponding author (okolibj@binghamuni.edu.ng)

Corrosion inhibitors sourced from greener agents are considered environmentally benign, with effective corrosion inhibition ability [14–16]. Plant-based polyphenols have been documented as having the ability to inhibit corrosion [17]. They are capable of donor-acceptor interactions using the oxygen lone pair electrons of the multiple aromatic hydroxyl groups and the metal surface [17], to form organometallic surface complexes that cling to the steel surface preventing the corrosion process [18].

A known natural source of polyphenols is the stem bark of the plant *Senegalia senegal*. Brittoncommonly known as gum arabic tree and widely distributed across the dry savannah and sahel regions. It is a drought tolerant shrub naturally distributed in Northern Nigeria which has been shown to contain reasonable amounts of corrosion inhibitor agents [19, 20]. Several studies, have been focused on the corrosion inhibition potentials of plant-based crude extract but none has been targeted on a specific class of phytochemical. Anand & Balasubramanian, [21] *i*nvestigated the corrosion behaviour of mild steel in acidic medium in presence of aqueous extract of *Allamanda blanchetii*. The study demonstrated the potential of *A. blanchetii* extract as a green and effective corrosion inhibitor for mild steel in acidic environments. This finding has implications for various industrial applications where corrosion protection of mild steel is crucial, such as in oil and gas, chemical processing, and construction industries. Another author Garg et al., [22] evaluated the Corrosion inhibition of copper by natural occurring plant *Acacia senegal*. The study demonstrated the potential of *A. senegal* extract as a green and effective corrosion inhibitor for copper in acidic environments. This finding has implications for various industrial applications where corrosion protection of copper is crucial, such as in electronics, automotive, and construction industries. This study aimed to evaluate the effectiveness of a polyphenol-rich fraction extracted from the stem bark of *S. senegal* as a corrosion inhibitor for mild steel in an acidic environment. The study investigated the influence of different temperatures and concentrations of the extract on its inhibition efficiency.

2. Methodology

2.1 Preparation of Mild Steel Test Coupons (MSTC)

The study employed mild steel sheets, which were transformed into test coupons measuring 2 cm x 2 cm x 0.1 cm. To achieve a smoother surface, emery paper was used to grade the surfaces. The graded test coupons were then subjected to a cleaning process using acetone to eliminate impurities. After air-drying, the cleaned test coupons were stored in a desiccator for elemental analysis and corrosion testing.

2.2 Extraction of *S. senegal* stem bark

2.2.1 Crude extraction by maceration

The stem barks of *S. senegal* were sourced from the Herbarium of the Botany section, Department of Biological Sciences, Ahmadu Bello University, Zaria, Kaduna State, with the voucher number ABU0332. The barks underwent a thorough washing process, followed by air-drying and pulverization to a particle size of 75 μm. Crude extraction was achieved through maceration, involving the complete immersion of 100 g of pulverized *S. senegal* stem bark in 200 ml of 70% acetone in a Winchester bottle. The bottle was then placed on a mechanical shaker at a temperature of 32 °C for a duration of four days. The extract was separated from the acetone using a Soxhlet evaporator (349/2 Wisetherm, China) under vacuum conditions at a temperature of 40 °C, as outlined in the study by Benali et al. [23]. The 30% water used in the extraction process was subsequently removed using a freeze-dryer (Cole Parmer 79203-00, USA). The resulting solid mass was stored in an airtight container for fractionation, by Solid Phase Extraction (SPE) clean-up. The percentage yield was determined using (1), which calculates the percentage of obtained extract relative to the dry weight of the stem bark.

$$\text{Percentage yield } = \frac{\text{amount of tannins obtained (g)}}{\text{amount of dry stem bark (g)}} x\ 100\%. \tag{1}$$

2.2.2 Solid Phase Extraction (SPE) clean-up of the extract

To start, a 100 mg size SPE cartridge is activated using 5 mL of methanol and then 5 mL of water. Next, a polyphenol-rich fraction (dissolved in water) of 50 mL is loaded onto the cartridge. To remove impurities, the cartridge is washed with 5 mL of 5% methanol. The elution process is done at a flow rate of 2 mL/min, using 5 mL of 80% acetonitrile. The eluates collected from this process are then concentrated using a rotary evaporator.

2.2.3 Qualitative and quantitative phytochemical screening of polyphenol fraction

Prepare a small amount of the sample polyphenol eluate and take a few drops of the eluate and transfer them to a test tube. Add 1% dilute ferric chloride solution to the test tube and observe the colour change in the solution. If polyphenols

are present, a colour change will occur due to the formation of coordination complexes between the phenolic compounds and ferric ions [24].

According to a modified method based on Wadhai et al., [25], the tannin content was determined by conducting several steps. Initially, 0.5 g of the powdered polyphenol sample was weighed and transferred to a test tube. Subsequently, 10 ml of distilled water was added and thoroughly mixed. Following this, 1 ml of Folin-Ciocalteu reagent was added to the solution and mixed well. After a duration of 5 minutes, 7.5 ml of a sodium carbonate solution (20% w/v) was added. The mixture was then allowed to stand in darkness for a period of 90 minutes, during which it developed a bluish-green color. To measure the absorbance of the resulting blue color, a double beam Shimadzu Ultraviolet (UV) spectrophotometer was used at a wavelength of 750 nm. Additionally, a calibration curve was prepared utilizing a standard tannic acid solution in order to calculate the tannin content of the sample.

A portion of 0.5 g of powdered polyphenol sample was added to a test tube. To the test tube, 10 ml of distilled water was added and the contents were thoroughly mixed using a vortex mixer or shaking manually. A volume of 1 ml of Folin-Ciocalteu reagent was introduced to the test tube and mixed well with the sample. The mixture was allowed to stand at room temperature (32°C) for 5 minutes to permit color development. After the 5-minute incubation period, 7.5 ml of a 2% w/v sodium carbonate solution was added to the test tube and a thorough mixing was ensured. The test tube was then placed in a water bath set at 40°C for 90 minutes to allow the reaction to complete. After the 90-minute incubation, the test tube was removed from the water bath. The resulting blue color in the test tube was measured for absorbance at 750 nm using a double beam UV spectrophotometer. A blank solution, consisting of distilled water, Folin-Ciocalteu reagent, and sodium carbonate solution, was prepared and its absorbance was measured as a reference. A calibration curve was prepared using a standard gallic acid solution, and its absorbance at 750 nm was measured for various concentrations. The total phenolic content of the polyphenol fraction was calculated by comparing the absorbance value of the sample to the calibration curve. The total phenolic content was expressed as milligrams of gallic acid equivalents per gram (mg GAE/g) of the polyphenol sample.

According to the report, the total phenolic content was determined by first checking the color stability of the polyphenol fraction at pH 4.5. The extract was added to separate test tubes, and the pH was adjusted using a 0.1 M hydrochloric acid solution. After observing the color changes, it was determined that pH 4.5 yielded the most stable color. A citric acid-sodium citrate buffer solution at pH 4.5 was prepared. A double beam Ultraviolet (UV) spectrophotometer was used to measure the absorbance of the resulting blue color at wavelengths of 520 nm and 700 nm. These wavelengths corresponded to the absorption maxima and minima of anthocyanins, respectively. The anthocyanin content in the polyphenol fraction was calculated using the following formula based on the differences in absorbance at the two wavelengths:

$$\text{Anthrocyanin content } \left(\frac{mg}{L}\right) = \frac{(\text{A} \times \text{MW} \times \text{DF})}{(\varepsilon \times \text{l})}, \tag{2}$$

where: A represents the absorbance difference between the two wavelengths (ΔA = A520 - A700), MW is the molecular weight of the anthocyanin compound, DF is the dilution factor if applicable, ε is the molar absorptivity of the specific anthocyanin compound, and l is the cuvette path length.

To determine the molar absorptivity (ε), a calibration curve was prepared using known concentrations of standard anthocyanin compounds. The absorbance of the standard solutions at both wavelengths was measured, and a graph of concentration against absorbance difference was plotted. The slope of the calibration curve represented ε.

2.3 Preparation of corrosion test media

A measured quantity of 0.2 g of the polyphenol fraction was dissolved in 1000 ml of 1M H_2SO_4 to obtain a concentration of 0.2 g/L. In addition, solutions of the polyphenol fraction were prepared at concentrations of 0.4, 0.6, and 0.8 g/L. To serve as the blank solution, an aqueous solution of 1M H_2SO_4 was prepared [26].

2.4 Gravimetric (weight loss) measurements

To measure weight loss for the purpose of weight loss, mild steel test coupons were initially weighed and then immersed individually in 50 ml of 1M H_2SO_4 in the presence and absence of a polyphenol fraction (inhibitor). The inhibitor concentrations used were 0.2, 0.4, 0.6, and 0.8 g/L, and the immersion took place in a 100 ml beaker at different temperatures of 30, 40, 50, and 60 $^{\circ}C$ for a duration of 6 hours [27]. After the immersion, the mild steel test coupons were removed, dried, and weighed using an analytical weighing balance (A$R^2$140 Adventurer, Illinois, USA). The corrosion rate ($\text{mgcm}^{-2}\text{h}^{-1}$), percentage inhibitor efficiency (IE%), and degree surface coverage (θ) were then calculated using (3), (4), and (5) respectively, as described by Adejoro et al. [28].

$$\text{Corrosion rate} = \frac{24\text{W}}{\text{AT}}, \tag{3}$$

where W = weight loss in grams; T = immersion time in hours; A = Area of mild steel test coupon in square cm (cm^2)

$$\text{IE\%} = 1 - \frac{\text{W1}}{\text{W2}} \text{x } 100, \tag{4}$$

$$\text{Degree surface coverage}(\theta) = 1 - \frac{\text{W1}}{\text{W2}}, \tag{5}$$

where W_1 = weight loss of mild steel coupon with inhibitor in acidic medium and W_2 = weight of mild steel coupon without inhibitor in acidic medium.

2.5 Adsorption and thermodynamic quantities

To explain the process of adsorption of polyphenol fraction (inhibitor) on the mild steel test coupon, the degree of surface coverage calculated from gravimetric studies were fitted into an empirical model of Langmuir, Freundlich and El-Awady isotherms using (6) – (8) according to [28, 29]:

Langmuir isotherm is given as;

$$\frac{\text{C}}{\theta} = \frac{1}{\text{K}_{\text{ads}}} + \text{C}, \tag{6}$$

where θ = degree surface coverage; C = inhibitor concentration; and K_{ads} = equilibrium constant of the adsorption process.

Freundlich isotherm is given as;

$$\text{Log } \theta = \text{Log K} + \frac{1}{\text{n}} \text{Log C}, \tag{7}$$

where θ = degree surface inhibition, $\frac{1}{\text{n}}$ = slope; Log K = intercept.

El-Awady Isotherm is given as;

$$\text{Log} \frac{\theta}{1-\theta} = \text{Log k} + \text{y Log C}, \tag{8}$$

where θ = degree surface inhibition; K is the isotherm constant; y is the number of inhibitor compound.

The thermodynamic parameters were determined according to (9) - (12):

Equilibrium constant of adsorption:

$$(K_{ads}) = \frac{\theta}{[\,(1-\theta)\,\text{C}]}, \tag{9}$$

where θ = degree surface coverage, C = inhibitor concentration, and K_{ads} = equilibrium constant of the adsorption process.

Gibbs free energy of adsorption ($\triangle G^{\circ}_{ads}$) is given as

$$\triangle G^{\circ}_{ads} = -2.303 RT Log(55.5 K_{ads}), \tag{10}$$

where R is the molar gas constant (8.314 kJ/mol), T is the temperature in Kelvin, and K_{ads} = equilibrium constant of the adsorption process.

Enthalpy of adsorption (Q_{ads}) is given as;

$$Q_{ads} = 2.303 R [Log \frac{\theta 2}{1-\theta 2} - Log \frac{\theta 1}{1-\theta 1}] x \frac{\text{T2T1}}{\text{T2} - \text{T1}}, \tag{11}$$

where R is the molar gas constant (8.314 kJ/mol), T_1 = represents temperatures 303 K, T_2 represents temperatures 323 K, θ_1 represents degree of surface coverage at T_1, and θ_2 represents degree of surface coverage at T_2.

Adsorption Activation Energy (E_a) is given as;

$$Log \frac{\text{CR}^2}{\text{CR1}} = \frac{\text{Ea}}{2.303\text{R}} \left[\frac{\text{T2} - \text{T1}}{\text{T1T2}} \right], \tag{12}$$

where R is the molar gas constant (8.314 kJ/mol), T_1 = represents temperatures 303 K, T_2 represents temperatures 323 K, CR_1 represent corrosion rate at T_1, and CR_2 represents corrosion rate at T_2.

2.6 Potentiodynamic polarization measurement

The potentiodynamic polarization measurement was conducted in a freshly prepared acidic blank solution as well as in solutions containing different concentrations (0.2, 0.4, 0.6, and 0.8 g/L) of the polyphenol fraction (inhibitor). The measurements were performed at a constant temperature of 30 ± 0.1 °C using a potentiostat device (ASTM G-61, Pennsylvania, USA). The device used a 3-electrode setup consisting of a reference electrode, a counter electrode, and a working electrode. In this case, the mild steel test coupon (MSTC) under investigation served as the working electrode. The potentiodynamic current-potential curves were recorded under experimental conditions including a set potential of 2.00 V, a scan rate of 0.10

V per second, and an interval time of 0.167 seconds [30]. The values of I_{corr} obtained from the anodic and cathodic curves of the Tafel plot were used to calculate the percentage inhibitor efficiency (%IE) using (13) [31]:

$$IE\% = 1 - \frac{Icorr(inh)}{Icorr(blk)} x\ 100, \tag{13}$$

where $I_{corr(inh)}$ is the corrosion current density in the inhibited medium and $I_{corr(blk)}$ is the corrosion current density in the uninhibited medium.

2.7 Characterization of polyphenol fraction and mild steel test coupon (MSTC)

The polyphenol fraction (inhibitor) was analyzed for its functional group composition using FT-IR. The scanning was done in the range of 4000 to 400 cm^{-1} using a PerkinElmer Spectrum 400 instrument. The surface morphology of the samples was observed using a Jeol JSM-6400 emission electron microscope. The thermal properties of the composites were determined through thermal gravimetric analysis (TGA 4000). The composites were subjected to a heating rate of 10 °C/min under a nitrogen flow (100 mL/min) from ambient temperature to 900 °C. The mass loss and calorific changes were recorded and plotted as thermal gravimetric (TG) and derivative thermal gravimetric (DTG) curves. The same procedure was followed for the MSTC samples.

3. Results and Discussion

3.1 Quantitative Analysis of Polyphenol-Rich Fraction of *S. Senegal* (PRFSS)

The phytochemical screening of polyphenol fraction (inhibitor) revealed the presence of tannins, phenols, and anthocyanins. The concentration of tannins was found to be 23.81 mg/100g, while the concentration of phenols and anthocyanins was 865.84 mg/100g and 90.04 mg/100g respectively (Table 1).

These findings are supported by previous research, which has shown that *S. senegal* is a rich source of polyphenols which is in agreement with the study by Sow, [32] found that the *S. senegal* contains a variety of phenolic compounds, including gallic acid, catechin, and epicatechin. Another study by Ex & Senthilkumar, [33] found that the polyphenol fraction (inhibitor) contains a high concentration of 865.84.

Phytochemical Constituents	Sample Concentration (mg/100g)
Tannins	23.81
Total Phenol	865.84
Anthocyanins	90.04

Table 1: Quantitative phytochemical screening of polyphenol fraction

Tannins, phenols, and anthocyanins can also form complexes with metal ions, which can prevent them from interacting with the surface of metal and causing corrosion. The presence of these polyphenol fractions suggests that it may have potential as a natural corrosion inhibitor [34–36].

3.2 FT-IR spectrum of Polyphenol-Rich Extract of *S. Senegal* (PRFSS)

The spectrum of PRFSS (Figure 1) shows a broad peak at 3209 cm^{-1}, which is characteristic of O-H stretching vibrations of phenolic compounds. The peak at 2118 cm^{-1} is due to C-C stretching vibrations of aromatic rings. The peak at 1611 cm^{-1} is due to C=O stretching vibrations of carbonyl groups. These peaks are all indicative of the presence of polyphenol in the extract.

The spectrum is similar to the tannin extract of *Acacia nilotica* with a broad peak at 3384 cm^{-1}, which is characteristic of O-H stretching vibrations of phenolic compounds. The peak at 2118 cm^{-1} is due to C-C stretching vibrations of aromatic rings. The peak at 1608 cm^{-1} is due to C=O stretching vibrations of carbonyl groups. These peaks are all indicative of the presence of tannins in the extract.

The spectra of polyphenol-rich extracts can be used to identify the type of polyphenols present in the extract. According to a study by El-Seedi et al., [37], FTIR spectroscopy was used to identify the types of polyphenols present in pomegranate peel extracts. They found that the spectra of the extracts contained a peak around 1500-1600 cm-1, which is indicative of the presence of ellagitannins.

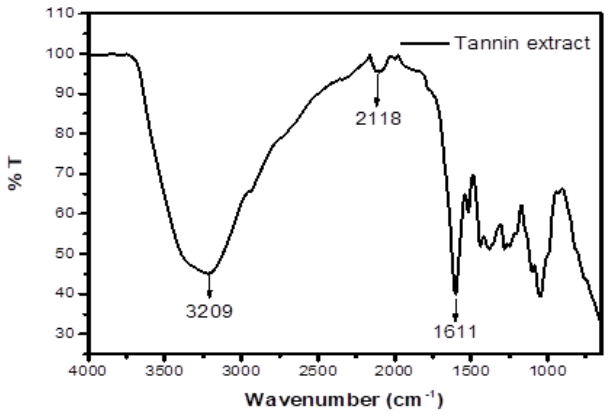

Figure 1: FTIR spectrum of polyphenol fraction

3.3 Thermal Stability of Polyphenol-Rich Fraction of *S. Senegal* (PRFSS)

The TGA and DTG curves of PRFSS are shown in Figure 2. The TGA curve shows that the extract undergoes two main stages of decomposition. The first stage occurs between 100 and 250°C, with a weight loss of about 10%. This stage is attributed to the loss of moisture from the extract. The second stage occurs between 300 and 500°C, with a weight loss of about 60%. This stage is attributed to the decomposition of the organic matter in the extract.

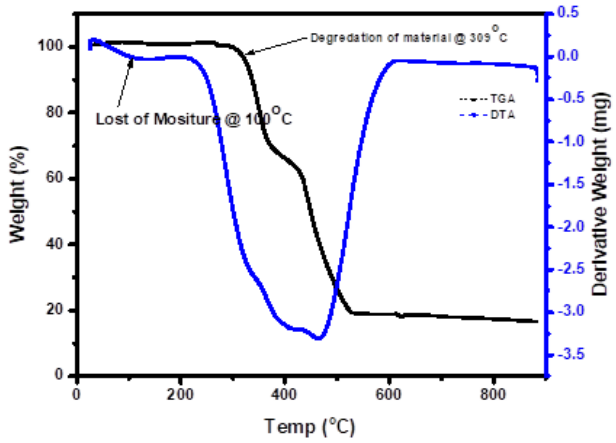

Figure 2: TGA and DTG profiles of Polyphenol-Rich Extract of S. Senegal (PRFSS)

The DTG curve shows that the rate of weight loss is highest between 300 and 400°C. This indicates that the decomposition of the organic matter in the extract occurs most rapidly in this temperature range.

The TGA and DTG curves of tannin rich extract of S. Senegal are similar to those of other plant materials. For example, the TGA curve of tannin rich extract of S. Senegal is similar to that of tannin rich extract of Acacia nilotica, which also undergoes two main stages of decomposition. The first stage occurs between 100 and 250°C, with a weight loss of about 10%, and the second stage occurs between 300 and 500°C, with a weight loss of about 60%. The DTG curve of tannin rich extract of S. Senegal is also similar to that of tannin rich extract of A. nilotica, which shows that the rate of weight loss is highest between 300 and 400°C.

3.4 Elemental Analysis of Mild Steel Test Coupon (MSTC)

Table 2 presents the XRF analysis result, revealing the elemental composition of the mild steel Test Coupon. The results clearly demonstrate a significant presence of iron (Fe), alongside the presence of other elements including aluminium, silicon, carbon, and cobalt. According to a study by Saxena & Mishra, (2019), iron (Fe) is an essential element in mild steel composition, as it provides strength and durability. Aluminium is known for its ability to improve the corrosion resistance of steel [38]. Silicon is commonly used as a deoxidizer, playing a crucial role in improving the mechanical properties of steel [39]. Carbon, as an integral part of steel, determines its hardness and strength [40]. Cobalt, although present in

relatively smaller quantities, can enhance the strength and high-temperature properties of steel [41]. Therefore, the XRF analysis, as presented in Table 2, aligns with the existing literature regarding the elemental composition of mild steel.

Element	Fe	C	Al	Si	Co
Composition (%)	89.044	1.890	4.418	4.162	0.292

Table 2: Elemental Composition of Mild Steel Test Coupon (MSTC)

3.5 Effect of PRFSS Concentration on Corrosion Rate and Surface Coverage of MSTC

The effect of increasing PRFSS concentration on corrosion rate and surface coverage of mild steel in 0.5M H_2SO_4 as temperature increases from 30 - 60^{o}C is shown in figure 3 (a-d). It can be seen that the corrosion rate decreases with increasing extract concentration. This is due to the fact that the extract contains polyphenols, which are known to be effective corrosion inhibitors. Polyphenolic compounds can form a protective layer on the metal surface, thereby preventing the metal from coming into contact with the corrosive environment. The surface coverage increases with increasing extract concentration, which further confirms the formation of a protective layer on the metal surface.

The results of this study are consistent with the study by Ebenso et al., [42] found that *Psidium guajava* extract was an effective corrosion inhibitor for mild steel in 0.5M H_2SO_4. The study found that the corrosion rate of mild steel decreased with increasing PRFSS concentration, and that the surface coverage of mild steel increased with increasing *S. Senegal* extract concentration. The protective layer is more effective at higher concentrations of *S. Senegal* extract, which results in a higher surface coverage.

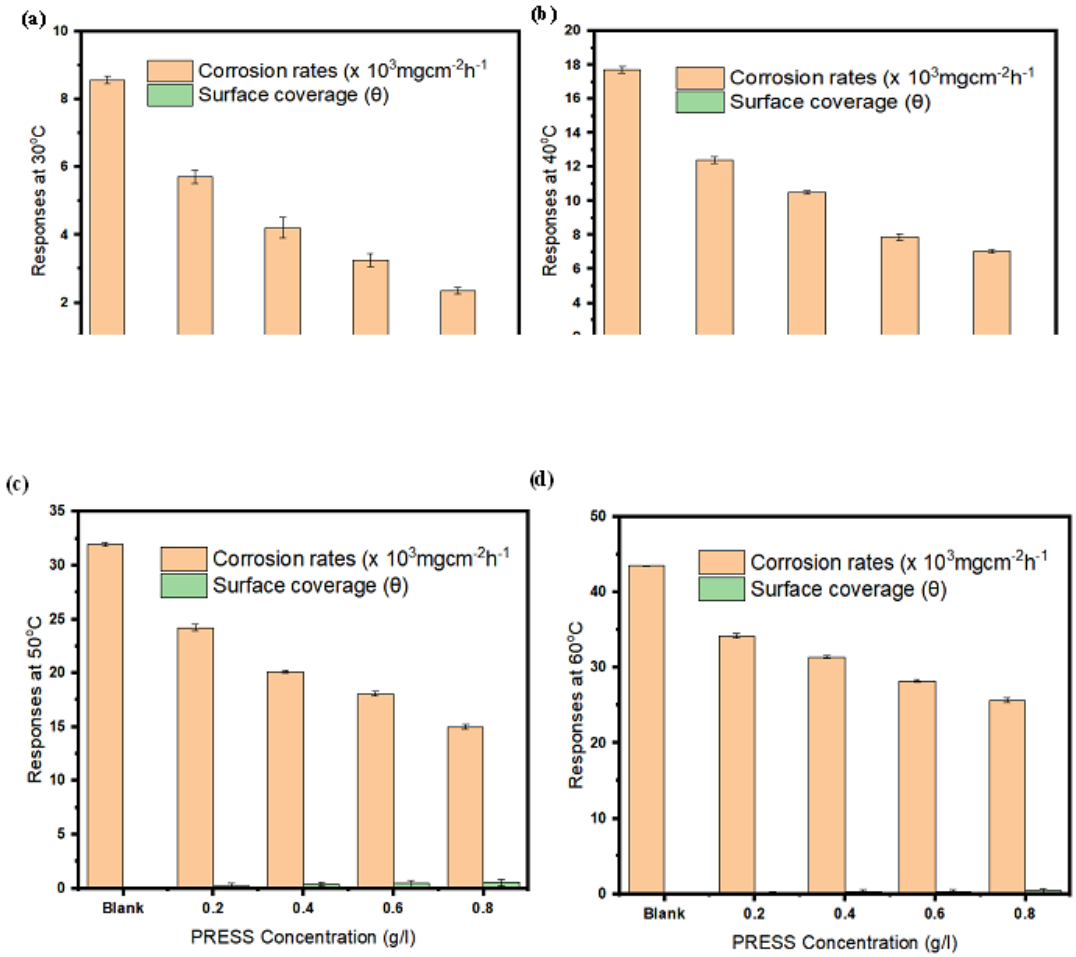

Figure 3: Calculated values of corrosion rates and surface coverage at (a) 30 °C, (b) 40 °C, (c) 50 °C, and (d) 60 °C for MSTC Corrosion in 1M H_2SO_4 and PRFSS inhibitor

Another study by Oguzie et al., [43] found that *P. guajava* extract was effective in inhibiting the corrosion of mild steel in saline solution. The authors found that the extract was able to form a protective layer on the metal surface, which prevented the metal from coming into contact with the corrosive environment. Further, Okafor et al., [44] found that *P. guajava* extract was effective in reducing the corrosion rate of mild steel in alkaline media. The results of this study suggest

that *S. Senegal* extract is a promising natural corrosion inhibitor for mild steel. The extract is effective in reducing the corrosion rate of mild steel in both acidic and alkaline media. The extract is also non-toxic and biodegradable, making it an environmentally friendly alternative to traditional corrosion inhibitors. The study found that the extract reduced the corrosion rate by up to 90%. A reduction in corrosion rate by up to 80% in mild steel was reported for *P. guajava* extract in 0.5 M H_2SO4 solution by Umoren et al., [45].

In figure 3 (a-d), it can be observed that the corrosion rate of mild steel in the blank solution (without PRFSS) increases with increasing temperature. This is because the increase in temperature provides more energy for the corrosion reaction to occur, leading to a faster rate of metal dissolution.

The addition of PRFSS to the solution decreases the corrosion rate of mild steel. This is due to the presence of polyphenols in the extract, which act as corrosion inhibitors. These polyphenols form a protective layer on the metal surface, which prevents the metal from coming into contact with the corrosive species in the solution. As the concentration of PRFSS increases, the surface coverage of the metal increases, which leads to a decrease in the corrosion rate (Figure 3 (a-d)). The effect of temperature on the corrosion rate of mild steel in the presence of PRFSS is not as significant as the effect of concentration. This is because the protective layer formed by the polyphenols is able to withstand temperatures of 30 °C - 60 °C.

3.6 Inhibition Efficiency of PRFSS Inhibitor on MSTC

The effect of increasing temperature and increasing PRFSS concentration on percentage corrosion inhibition efficiency (% IE) of MSTC in 1M H_2SO_4 (Figure 4). It can be seen that the percentage corrosion inhibition efficiency increases with increasing concentration of PRFSS. This is because the extract contains compounds that act as corrosion inhibitors, and increasing the concentration of the extract increases the amount of these inhibitors present on the surface of the metal, which results in a higher degree of protection against corrosion.

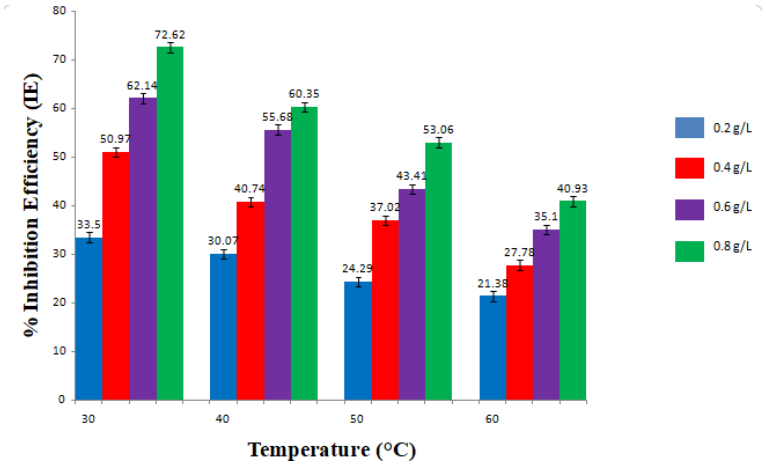

Figure 4: Percentage inhibition efficiency (%IE) of 0.2 g/L - 0.8 g/L PRFSS on MSTC in 1M H_2SO_4 at varying temperatures

The percentage corrosion inhibition efficiency also decreases with increasing temperature. This is because the increased temperature provides more energy for the corrosion reaction to occur, which overcomes the protective effect of the inhibitors.

The results of this study are consistent with those of Ebenso et al., [6] found that *P. guajava* extract inhibited the corrosion of mild steel in 1M HCl solution, and that the percentage corrosion inhibition efficiency increased with increasing concentration of the extract. According to Oguzie et al., [43], it was observed that the presence of *P. guajava* extract inhibited the corrosion of mild steel in a solution of 0.5M H_2SO_4. The study also revealed that the effectiveness of corrosion inhibition, exPRFSSed as the percentage of corrosion inhibition efficiency, was positively correlated with the concentration of the extract. On the contrary, as temperature increased, the corrosion inhibition efficiency decreased.

3.7 Adsorption and Thermodynamics Considerations

3.7.1 Langmuir adsorption model

In Table 3, the adsorption of PRFSS onto mild steel, the Langmuir model provides a good fit to the experimental data, with a R^2 values between 0.963 - 0.993. The maximum adsorption capacities of the mild steel surface as temperature increases from 30°C to 60°C results in increase in equilibrium constant is found to be 0.84 -1.63 L/g. This indicates that the PRFSS has a strong affinity for the MSTC surface and that the adsorption process is reversible.

The model's prediction is supported by the observation that the maximum coverage and absorption coefficient increase as the temperature increases. This suggests that the process of adsorption of PRFSS onto MSTC is a physisorption process, involving weak van der Waals forces between the adsorbate and the adsorbent. Furthermore, at higher temperatures, the extract molecules are more strongly attracted to the MSTC surface.

Other studies have also found that the Langmuir adsorption model effectively describes the adsorption of *S. senegal* extract onto various metal surfaces. In the study conducted by Jouhari et al., [46], it was established that the Langmuir adsorption model is suitable for describing the adsorption of *S. senegal* extract onto copper. Similarly, another study by Jouhari et al., [47] concluded that the Langmuir adsorption model accurately represents the adsorption of *S. senegal* extract onto aluminum.

	Temperature 30^{o}C				Temperature 40^{o}C			
PRFSS Conc. (g/L)	Surface coverage ($\boldsymbol{\theta}$)	C/$\boldsymbol{\theta}$	R^2	Slope	Surface coverage ($\boldsymbol{\theta}$)	C/$\boldsymbol{\theta}$	R^2	Slope
Blank	-	-	0.993	0.84	-	-	0.963	1.04
0.2	0.34	0.5882			0.30	0.6700		
0.4	0.51	0.7843			0.41	0.9818		
0.6	0.62	0.9677			0.56	1.0714		
0.8	0.73	1.0959			0.60	1.3333		
	Temperature 50^{o}C				Temperature 60^{o}C			
PRFSS Conc. (g/L)	Surface coverage ($\boldsymbol{\theta}$)	C/$\boldsymbol{\theta}$	R^2	Slope	Surface coverage ($\boldsymbol{\theta}$)	C/$\boldsymbol{\theta}$	R^2	Slope
Blank	-	-	0.970	1.16	-	-	0.97	1.63
0.2	0.24	0.8333			0.21	0.9524		
0.4	0.37	1.0811			0.28	1.4420		
0.6	0.43	1.3954			0.35	1.7094		
0.8	0.53	1.5094			0.41	1.95122		

Table 3: Langmuir adsorption model values for MSTC in 1M H_2SO_4 and 0.2-0.8 g/L PRFSS inhibitor concentration at 30, 40, 50, and 60 °C.

3.7.2 Freundlich adsorption model

The Freundlich adsorption model of the plot of log of PRFSS concentration against log θ of MSTC shows a general increase in temperature with decrease adsorption capacity and heterogeneity of adsorbent surface (Figure 4). In the case of the adsorption of PRFSS on MSTC, the Freundlich adsorption model was found to fit the data well, with a R^2 values between 0.980 - 0.991. The values of the Freundlich constant, K, and the Freundlich exponent, n, were found to be 0.48 - 0.7 and 1.79 - 2.08, respectively. This indicates that the adsorption of PRFSS on MSTC is a heterogeneous process and that the adsorbent has a high adsorption capacity.

	Temperature 30oC					Temperature 40oC				
PRFSS Conc. (g/L)	Surface coverage (θ)	Log C	Log θ	R^2	Slope	Surface coverage (θ)	Log C	Log θ	R^2	Slope
Blank	-	-	-			-	-	-		
0.2	0.34	-0.6990	-0.4685			0.2985	-0.6990	-0.5251		
0.4	0.51	-0.3979	-0.2924	0.998	0.55	0.4074	-0.3979	-0.3810	0.980	0.53
0.6	0.62	-0.2219	-0.2076			0.56	-0.2219	-0.2518		
0.8	0.73	-0.0969	-0.1367			0.6	-0.0969	-0.2219		
	Temperature 50oC					Temperature 60oC				
PRFSS Conc. (g/L)	Surface coverage (θ)	Log C	Log θ	R^2	Slope	Surface coverage (θ)	Log C	Log θ	R^2	Slope
Blank	-	-	-			-	-	-		
0.2	0.24	-0.6990	-0.6198			0.21	-0.6990	-0.6778		
0.4	0.37	-0.3979	-0.4318	0.991	0.56	0.27	-0.3979	-0.5569	0.991	0.48
0.6	0.43	-0.2219	-0.3665			0.35	-0.2219	-0.4547		
0.8	0.53	-0.0969	-0.2757			0.41	-0.0969	-0.3872		

Table 4: Freundlich adsorption model values for MSTC in 1M H_2SO_4 and 0.2-0.8 g/L PRFSS concentration at 30, 40, 50, and 60 °C

3.7.3 El-Awady adsorption model

The experimental data in Table 5 are consistent with the predictions of the El-Awady adsorption model. The surface coverage of the MSTC by PRFSS increases with increasing PRFSS concentration and temperature. The slope of the plot

of log of PRFSS concentration against log (θ/1-θ) also increases with increasing temperature.

According to El-Awady et al., [48], it was found that this adsorption model can be used to describe the adsorption of other solutes onto other solid surfaces; as described in the adsorption of methylene blue onto activated carbon. Another study by El-Khaiary et al., [49] found that the adsorption model could be used to describe the adsorption of phenol onto silica gel.

	Temperature 30oC					Temperature 40oC				
PRFSS Conc. (g/L)	Surface coverage (θ)	Log C	Log θ/1-θ	R^2	Slope	Surface coverage (θ)	Log C	Log θ/1-θ	R^2	Slope
Blank	-	-	-			-	-	-		
0.2	0.34	-0.6990	-0.2881			0.2985	-0.6990	-0.3711		
0.4	0.51	-0.3979	0.0174	0.986	1.16	0.4074	-0.3979	-0.1627	0.970	0.95
0.6	0.62	-0.2219	0.2126			0.56	-0.2219	0.1047		
0.8	0.73	-0.0969	0.4320			0.6	-0.0969	0.1761		
	Temperature 50oC					Temperature 60oC				
PRFSS Conc. (g/L)	Surface coverage (θ)	Log C	Log θ/1-θ	R^2	Slope	Surface coverage (θ)	Log C	Log θ/1-θ	R^2	Slope
Blank	-	-	-			-	-	-		
0.2	0.24	-0.69897	-0.5006			0.21	-0.69897	-0.57541		
0.4	0.37	-0.39794	-0.23114	0.986	0.88	0.2774	-0.39794	-0.41579	0.983	0.69
0.6	0.43	-0.22185	-0.12241			0.351	-0.22185	-0.26694		
0.8	0.53	-0.09691	0.052178			0.41	-0.09691	-0.15807		

Table 5: El-Awady adsorption model values for MSTC in 1M H_2SO_4 and 0.2-0.8 g/L PRFSS concentration at 30, 40, 50, and 60 °C

3.7.4 Equilibrium constant of adsorption (K_{ads}) and Gibbs free energy ($\triangle G_{ads}$)

The thermodynamic-kinetic equilibrium constant of adsorption (K_{ads}) measures the effectiveness of the adsorption interaction between the PRFSS inhibitor adsorbent molecule and the adsorbate (Table 6). The decrease in equilibrium constant of adsorption (K_{ads}) with increasing temperature suggests that the adsorption process is exothermic in nature. This means that the adsorption of PRFSS on the MSTC surface is more favorable at lower temperatures. The decrease in K_{ads} with increasing PRFSS concentration can be attributed to the saturation of the adsorption sites on the MSTC surface. At higher concentrations, there are more extract molecules competing for the same adsorption sites, resulting in a decrease in the number of molecules that are able to adsorb.

Temperature (℃)	30	40	50	60
Equilibrium constant of adsorption (K_{ads})	0.6439	0.5357	0.3947	0.3322
Gibbs free energy of adsorption (kJmol^{-1})	-8.02	-8.62	-9.50	-9.20

Table 6: Calculated values of K_{ads}, $\triangle G_{ads}$ (kJmol^{-1}) for MSTC dissolution in 1M H_2SO_4 and 0.2 g/L to 0.8 g/L PRFSS inhibitor concentration at 30 $°C$, 40 $°C$, 50 $°C$ and 60 $°C$

The decrease in Gibbs free energy of adsorption (ΔG_{ads}) with increasing temperature indicates that the adsorption process is spontaneous. The more negative the value of ΔG_{ads}, the more spontaneous the process. The decrease in ΔG_{ads} with increasing PRFSS concentration suggests that the adsorption process is more favorable at higher concentrations. This is because the higher the concentration of PRFSS, the more molecules there are available to adsorb on the MSTC surface, resulting in a greater decrease in ΔG_{ads}.

These results are consistent with those by Ebenso et al., [42] who found that the adsorption of *P. guajava* extract on mild steel in 0.5 M H_2SO_4 was exothermic and spontaneous. The decrease in K_{ads} and ΔG_{ads} with increasing temperature and inhibitor concentration were attributed to the saturation of the adsorption sites on the mild steel surface.

Another study by Oguzie et al., [43] found that the adsorption of *P. guajava* extract on mild steel in 1M H_2SO_4 was also exothermic and spontaneous. The decrease in K_{ads} and ΔG_{ads} with increasing temperature and inhibitor concentration were attributed to the formation of a protective layer on the mild steel surface. The decrease in K_{ads} and ΔG_{ads} with increasing temperature and PRFSS concentration in the inhibition of MTSC in 1M H_2SO_4 can be attributed to the exothermic nature of the adsorption process and the saturation of the adsorption sites on the MTSC surface.

3.7.5 Enthalpy of adsorption (Q_{ads}) and Activation energy (E_a)

Table 7 revealed an increase in enthalpy of adsorption (Q_{ads}) with increasing concentration of PRFSS which is likely due to the increased number of active sites on the extract surface that are available for interaction with the metal ions. The stronger

interaction between PRFSS and the MSTC surface leads to a decrease in the activation energy (E_a) for the dissolution of MSTC. This is because the extract molecules act as a barrier between the MSTC surface and the corrosive species in the solution, which makes it more difficult for the MSTC to dissolve.

PRFSS Concentration (g/L)	Blank	0.2	0.4	0.6	0.8
Activation energy (E_a)	45.73	50.08	55.84	60.49	66.92
Enthalpy of adsorption (Q_{ads})	-	-18.51	-26.42	-31.01	-38.01

Table 7: Calculated values of activation energy (E_a) and heat of adsorption (Q_{ads}) for MSTC dissolution in 1M H_2SO_4 and 0.2 to 0.8 g/L PRFSS inhibitor concentration at 30 $^\circ C$ and 60 $^\circ C$

The decrease in E_a with increasing PRFSS concentration has been reported by Abba-Aji et al., [50] found that the E_a for the dissolution of mild steel in 0.5M H2SO4 decreased from 75.8 kJ/mol to 58.9 kJ/mol with increasing concentration of *Vernonia amygdalina* extract.

The decrease in E_a with increasing inhibitor concentration can be explained by the fact that the inhibitor molecules compete with the corrosive species for adsorption sites on the metal surface. As the inhibitor concentration increases, the number of inhibitor molecules adsorbed on the surface increases, which decreases the number of sites available for the corrosive species. This leads to a decrease in the rate of dissolution and a decrease in the E_a.

3.8 Potentiodynamic Polarization Study

The polarization plot in Figure 5 shows the relationship between the potential of a metal electrode and the current density flowing through it, which is a useful tool for studying the corrosion behaviour of metals. The polarization plot shows that the Tafel slopes of MSTC in 0.6 g/L, 0.2 g/L, 0.4 g/L and 0.8 g/L PRFSS inhibitor are 128.9 mV/decade, 109.8 mV/decade, 90.7 mV/decade and 78.6 mV/decade, respectively, which indicates that the corrosion inhibition efficiency of PRFSS increases with increasing inhibitor concentration. This is because the inhibitor molecules adsorb onto the surface of the MSTC electrode and block the active sites for corrosion, thereby preventing the metal from corroding.

The corrosion current density of mild steel in acidic medium is 3.87E-05 A/cm^2, which is higher than that in 0.6 g/L (2.03E-05 A/cm2), 0.2 g/L (1.27E-05 A/cm2), 0.4 g/L (0.89E-05 A/cm2) and 0.8 g/L (0.67E-05 A/cm2) PRFSS inhibitor. This indicates that the PRFSS inhibitor is an effective corrosion inhibitor for mild steel in acidic medium.

The polarization curves of MSTC in different concentrations of PRFSS inhibitor are Tafel lines, which means that the corrosion rate is controlled by the charge transfer process. The Tafel slopes of MSTC in different concentrations of PRFSS inhibitor are close to each other, which indicates that the mechanism of corrosion inhibition of PRFSS inhibitor is the same at different concentrations.

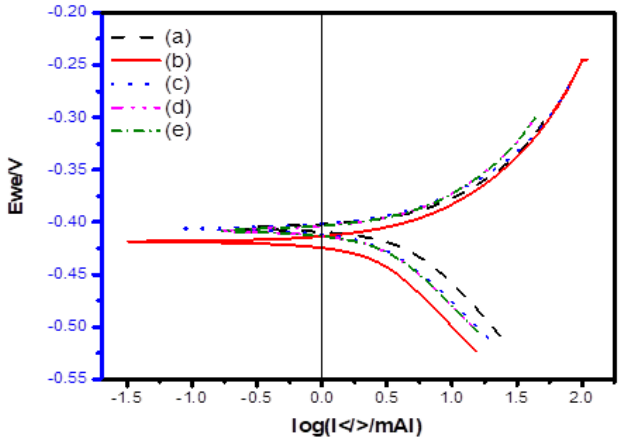

Figure 5: Polarization plot of MSTC in (a) 0.6 g/L, (b) an acidic medium, (c) 0.2 g/L, (d) 0.4 g/L, and (e) 0.8 g/L PRFSS inhibitors

The corrosion potential of MSTC in different concentrations of PRFSS inhibitor shifts to more positive values with increasing inhibitor concentration, which indicates that the PRFSS inhibits the corrosion of MSTC by catholic protection mechanism. The results of this study show that PRFSS is an effective corrosion inhibitor for mild steel in acidic medium. The corrosion inhibition efficiency of PRFSS increases with increasing inhibitor concentration. The PRFSS inhibitor inhibits the corrosion of MSTC by cathodic protection mechanism.

The potentiodynamic polarization parameters and increase inhibition efficiency for MSTC corrosion in 1M H_2SO_4 with increase in PRFSS inhibitor concentration at 32 $°C$ are shown in the table below.

Inhibitor Conc. (g/L)	E_{corr} (mV vs SCE)	I_{corr} (mA/cm^2)	ß$_a$ (mV/dec)	ß$_c$ (mV/dec)	%IE
Blank	-418.45	414.46	133.19	-119.87	-
0.2	-407.15	287.94	81.41	-82.41	30.54
0.4	-404.20	239.06	69.97	-76.22	42.34
0.6	-404.76	109.70	72.05	-75.17	73.53
0.8	-407.81	85.81	67.64	-71.89	79.30

Table 8: Calculated potentiodynamic polarization parameters and inhibition efficiency for mild steel corrosion in 1M H_2SO_4 and 0.2 to 0.8 g/L SSBT inhibitor concentration at 32 $°C$

As can be seen from the table 5, the corrosion potential (E_{corr}) of MSTC in 1M H_2SO_4 shifted towards more positive values with the addition of PRFSS inhibitor, which indicates that the inhibitor is anodic. The corrosion current density (Icorr) decreased with the increase of inhibitor concentration, which indicates that the inhibitor is effective in reducing the corrosion rate of MSTC. The Tafel slopes (βa and βc) increased with the increase of inhibitor concentration, which indicates that the inhibitor is a mixed-type inhibitor. The inhibition efficiency (%IE) increased with the increase of inhibitor concentration, which indicates that the inhibitor is effective in protecting MSTC from corrosion.

The results of this study are consistent with the findings of Odewunmi et al., [51] which showed that watermelon waste products were effective in reducing the corrosion rate of mild steel in HCl. The corrosion inhibition efficiency of PRFSS is likely due to the presence of polyphenols, which are known to be effective corrosion inhibitors. Polyphenolic compounds can form complexes with metal ions, which prevents them from reacting with oxygen and water to form corrosion products.

3.9 Characterisation of MSTC in 1M H_2SO_4 and PRFSS inhibitor

3.9.1 FT-IR analysis of MSTC After Corrosion Inhibition Study

The spectrum of MSTC in 1M H_2SO_4 shows a broad peak at around 3400 cm^{-1}, which is due to the stretching vibrations of O-H bonds in the adsorbed water molecules on the steel surface (Figure 6). The peak at around 1630 cm^{-1} is due to the bending vibrations of C=O bonds in the adsorbed CO_2 molecules. The peak at around 1030 cm^{-1} is due to the stretching vibrations of C-O bonds in the adsorbed CO_3^{2-} ions.

The spectrum of MSTC in PRFSS inhibitor shows a broad peak at around 3400 cm^{-1}, which is due to the stretching vibrations of O-H bonds in the adsorbed water molecules on the steel surface. The peak at around 1630 cm^{-1} is due to the bending vibrations of C=O bonds in the adsorbed CO_2 molecules. The peak at around 1030 cm^{-1} is due to the stretching vibrations of C-O bonds in the adsorbed CO_3^{2-} ions. In addition, there are two new peaks at around 1513 cm^{-1} and 2026 cm^{-1}, which are due to the stretching vibrations of C=C bonds and C-N bonds in the PRFSS inhibitor molecules.

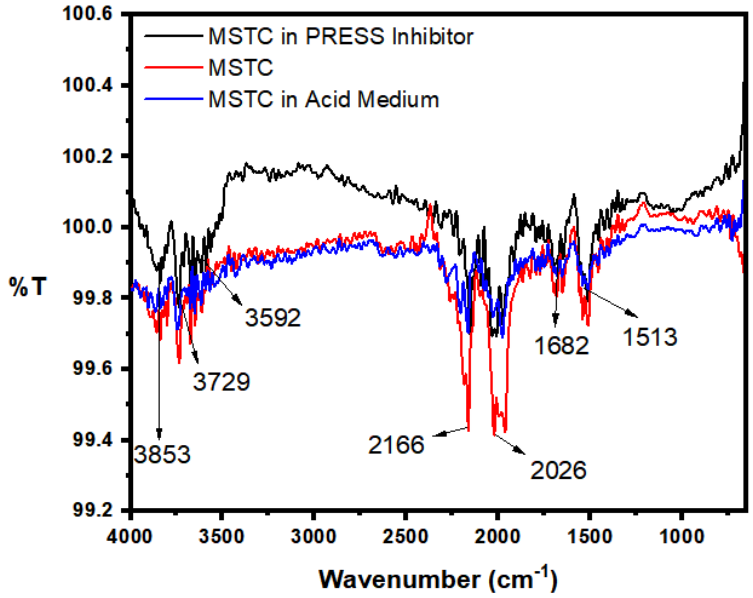

Figure 6: FTIR spectrum of MSTC (red), MSTC in 1M H_2SO_4 (blue), and MSTC in PRFSS inhibitor (black)

The spectrum shows that the PRFSS inhibitor is adsorbed on the MSTC surface, and that the inhibitor molecules are

bonded to the steel surface through the C=C and C-N bonds. This is consistent with the results of the potentiodynamic polarization curves (Figure 6), which showed that the PRFSS inhibitor is an effective corrosion inhibitor for mild steel in acidic media.

The comparison of the FTIR spectra of mild steel in acidic blank and PRFSS inhibitor shows that the inhibitor is adsorbed on the mild steel surface and forms a protective layer that prevents the metal from corroding. This is consistent with the results of the potentiodynamic polarization curves, which showed that the PRFSS inhibitor is an effective corrosion inhibitor for mild steel in acidic media.

3.9.2 Morphological Analysis of MSTC After Corrosion Inhibition Study

The SEM micrographs show the surface of MSTC, MSTC in 1M H_2SO_4, MSTC in 1M H_2SO_4, and PRFSS inhibitor (Figure 7(a-c)). The SEM micrograph in Figure 7(a) shows the surface of MTSC in blank with polished steel surface. The surface is slightly rough, but there are no pits or cracks, because the blank solution does not contain any corrosive agents.

The surface of MSTC in 1M $H_2SO_4$is rough and corroded, with many pits and cracks. This is because the acidic solution has dissolved the metal, leaving behind a rough and uneven surface (Figure 7(b)). The micrograph in Figure 7(c) shows the surface of MSTC in PRFSS inhibitor. The surface is much smoother and less corroded than the surface in figure 7(b) because the inhibitor has protected the metal from the corrosive effects of the acid. This protective layer is evident in the SEM micrograph as the smooth surface (Figure 7(c)).

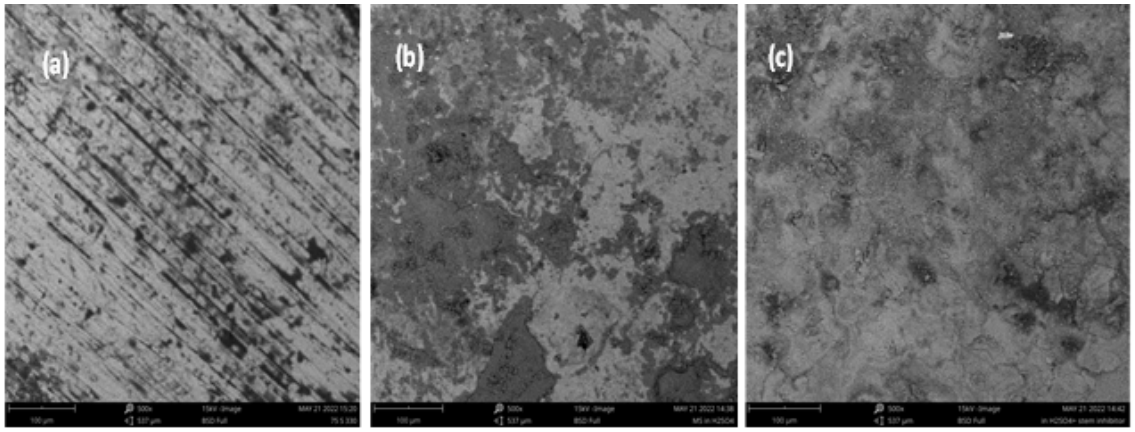

Figure 7: SEM images of mild steel test coupon at magnification of 500x

4. Conclusion

In this study, we evaluated the efficacy of a polyphenol-rich fraction (PRFSS) from *S. senegal* as a green corrosion inhibitor for mild steel in an acidic environment. The PRFSS was rich in tannins, phenols, and anthocyanins. The adsorption and thermodynamic studies indicated that the adsorption of PRFSS on the mild steel surface was a physisorption process, and that the process was spontaneous and exothermic. The potentiodynamic polarization study showed that the PRFSS inhibitor inhibited the corrosion of mild steel by cathodic protection mechanism. The PRFSS inhibitor was able to form a protective layer on the mild steel surface, which prevented the metal from coming into contact with the corrosive species in the solution. This study demonstrates the potential of PRFSS as a sustainable and environmentally friendly corrosion inhibitor for mild steel in acidic environments.

The results of the present study provide an eco-friendly approach to control the corrosion of mild steel in 1M H2SO4 solution. The inhibition efficiency of PRFSS was evaluated using electrochemical techniques. Thermodynamic parameters were used to examine the adsorption behaviour of the inhibitor on the mild steel in the acidic solution. The percentage inhibition efficiency (IE%) of the PRFSS was found to increase as its concentration increases. This behaviour is attributed to the formation of an organic protective layer on mild steel surface. The adsorption of the PRFSS inhibitor on mild steel is well fitted to the Langmuir adsorption model and its physicochemical interaction with the metal surface has been investigated by potentiodynamic polarisation method. The inhibition efficiency of the studied natural extract against the metal corrosion may be enhanced when used with other conventional corrosion inhibitors in future work.

Funding

This research received no external financial support for the publication of this work.

Data Availability Statement

The data used to support this study are available within the manuscript.

Acknowledgments

The authors greatly acknowledge the University central laboratory, Umaru Musa Yaradua University Katsina,PMB2218 (www.umyu.edu.ng) Katsina State, Nigeria and the Faculty of Engineering, Ahmadu Bello University Zaria, Nigeria for their discipline of excellence for performing the analyses for the research.

Conflicts of Interest

The authors have declared that there is no conflict of interest.

References

[1] Gayakwad, N., Patil, V., Rao, B. M., Gokale, G. M., & Gurlhosur, K. (2021). Studies on Rhoeo discolor plant extract as a natural corrosion inhibitor. *Journal of Environmental Engineering and Science, 16*(2), 66-76.

[2] Fouda, A. S., El-Defrawy, A. M., & El-Sherbeni, M. W. (2013). Lornoxicam & Tenoxicam Drugs as Green Corrosion Inhibitors for Carbon Steel in 1 M H 2 SO 4 Solution . *Journal of Electrochemical Science and Technology, 4*(2), 47-56.

[3] Adindu, C. B., Oguzie, E. E., & Chidiebere, M. A. (2016). Corrosion Inhibition and Adsorption Behavior of Extract of *Funtumia elastica* on Mild Steel in Acidic Solution. *International Letters of Chemistry, Physics and Astronomy, 66*, 119-132.

[4] Patni, N., Agarwal, S., & Shah, P. (2013). Greener Approach towards Corrosion Inhibition. *Chinese Journal of Engineering, 2013*, 1-10.

[5] Agresor, J. H., & Cui-lim, K. M. R. (2018). *Nypa fruticans (NIPA) starch filled with zinc oxide nanoparticles as corrosion inhibitor in steel. 54*(273).

[6] Dubey, R. S. (2020). Green Corrosion Inhibitos Formetals and Alloys: a Comprehensive Review. *International Journal of Advanced Research, 8*(6), 1558-1565.

[7] Oguzie, E. E., Enenebeaku, C. K., Akalezi, C. O., Okoro, S. C., Ayuk, A. A., & Ejike, E. N. (2010). Adsorption and corrosion-inhibiting effect of Dacryodis edulis extract on low-carbon-steel corrosion in acidic media. *Journal of Colloid and Interface Science, 349*(1), 283-292.

[8] Rajeswari, V., Kesavan, D., Gopiraman, M., Viswanathamurthi, P., Poonkuzhali, K., & Palvannan, T. (2014). Corrosion inhibition of Eleusine aegyptiaca and Croton rottleri leaf extracts on cast iron surface in 1 M HCl medium. *Applied Surface Science, 314*, 537-545.

[9] Atadious, D., & Ogie, N. (2021). *Controlling Induced-Corrosion in Oil pipelines : Determining the Inhibition Efficiency of Vernomiaamygdalina as a Natural Corrosion Inhibitor in comparison to Potassium Chromate Controlling Induced-Corrosion in Oil pipelines : Determining the Inhibition E. September.*

[10] Popoola, L. T. (2019). Progress on pharmaceutical drugs, plant extracts and ionic liquids as corrosion inhibitors. *Heliyon, 5*(2), e01143.

[11] Schweitzer, P. A. (2017). Corrosion inhibitors. *Corrosion and Corrosion Protection Handbook, Second Edition*, 47-52.

[12] Rani, B. E. A., & Basu, B. B. J. (2012). Green inhibitors for corrosion protection of metals and alloys: An overview. *International Journal of Corrosion, 2012*(i). https://doi.org/10.1155/2012/380217

[13] Marzorati, S., Verotta, L., & Trasatti, S. P. (2019). Green corrosion inhibitors from natural sources and biomass wastes. *Molecules, 24*(1).

[14] Da Rocha, J. C., Da Cunha Ponciano Gomes, J. A., & D'Elia, E. (2014). Aqueous extracts of mango and orange peel as green inhibitors for carbon steel in hydrochloric acid solution. *Materials Research, 17*(6), 1581-1587.

[15] Kaco, H., Talib, N. A. A., Zakaria, S., Jaafar, S. N. S., Othman, N. K., Chia, C. H., & Gan, S. (2018). Enhanced corrosion inhibition using purified tannin in HCL medium. *Malaysian Journal of Analytical Sciences, 22*(6), 931-942.

[16] Umoren, S. A., Eduok, U. M., Solomon, M. M., & Udoh, A. P. (2016). Corrosion inhibition by leaves and stem extracts of Sida acuta for mild steel in 1 M H2SO4 solutions investigated by chemical and spectroscopic techniques. *Arabian Journal of Chemistry, 9*, S209-S224.

[17] Abdulmajid, A., Hamidon, T. S., Rahim, A. A., & Hussin, M. H. (2019). Tamarind shell tannin extracts as green corrosion inhibitors of mild steel in hydrochloric acid medium. *Materials Research Express, 6*(10).

[18] Yetri, Y., Gunawarman, Emriadi, & Jamarun, N. (2018). Theobroma cacao Peel Extract as the Eco-Friendly Corrosion Inhibitor for Mild Steel. *Corrosion Inhibitors, Principles and Recent Applications.*

[19] Eldin, I., Elgailani, H., & Ishak, C. Y. (2016). *Methods for Extraction and Characterization of Tannins from Some Acacia Species of Sudan. 17*(1), 43-49.

[20] Omokhafe, K. O. (2014). *Morphological Study of Acacia senegal (L.) Willd. from Borno and Yobe States, Nigeria. 5*(8), 237-239.

[21] Anand, B., & Balasubramanian, V. (2011). Corrosion behaviour of mild steel in acidic medium in presence of aqueous extract of Allamanda blanchetii. *E-Journal of Chemistry, 8*(1), 226-230.

[22] Garg, U., Kumpawat, V., Chauhan, R., & Tak, R. K. (2011). Corrosion inhibition of copper by natural occurring plant Acacia senegal. *Journal of the Indian Chemical Society, 88*(4), 513-519.

[23] Benali, O., Benmehdi, H., Hasnaoui, O., Selles, C., & Salghi, R. (2013). Green corrosion inhibitor: Inhibitive action of tannin extract of Chamaerops humilis plant for the corrosion of mild steel in 0.5M H2SO4. *Journal of Materials and Environmental Science, 4*(1), 127-138.

[24] Banu, K. S., & Cathrine, L. (2015). General Techniques Involved in Phytochemical Analysis. *International Journal of Advanced Research in Chemical Science, 2*(4), 25-32.

[25] Wadhai, M., Ayate, D., & Ujjainkar, V. (2019). Estimation of tannin content in leaves, bark and fruits of *Terminalia arjuna* Roxb. *International Journal of Farm Sciences, 9*(1), 61.

[26] Rukaiyat, M. S., Abubakar, G. S., & Fatima, M. K. (2018). Corrosion inhibition of mild steel using alkaloids and tannins extracts of *Jatropha curcas* in acidic media. *Bayero Journal of Pure and Applied Sciences, 10*(1), 311.

[27] Talib, N. A. A., Zakaria, S., Hua, C. C., & Othman, N. K. (2014). Tannin bark melalauca cajuputi powell (Gelam) as green corrosion inhibitor of mild steel. *AIP Conference Proceedings, 1614*(February 2015), 171-177.

[28] Adejoro, I. A., Ojo, F. K., & Obafemi, S. K. (2015). Corrosion inhibition potentials of ampicillin for mild steel in hydrochloric acid solution. *Journal of Taibah University for Science, 9*(2), 196-202.

[29] Aralu, C. C., Chukwuemeka-Okorie, H. O., & Akpomie, K. G. (2021). Inhibition and adsorption potentials of mild steel corrosion using methanol extract of Gongronema latifoliuim. *Applied Water Science, 11*(2), 1-7.

[30] Peres, R. S., Cassel, E., & Azambuja, D. S. (2012). Black Wattle Tannin As Steel Corrosion Inhibitor. *ISRN Corrosion, 2012*, 1-9.

[31] Shah, A. M., Rahim, A. A., Yahya, S., Raja, P. B., & Hamid, S. A. (2011). Acid corrosion inhibition of copper by mangrove tannin. *Pigment and Resin Technology, 40*(2), 118-122.

[32] Sow, D. (2014). Antioxidant and antimicrobial activities of polyphenols from Senegalia senegal stem bark. *Industrial Crops and Products, 61*, 438-447.

[33] Ex, S. R. B., & Senthilkumar, S. M. (2015). Phytochemical Screening and Antibacterial Activity of Gymnema. *International Journal of Pharmaceutical Sciences and Research IJPSR, 6*(6), 2496-2503.
[34] Ebenso, E., Ibhadode, A., Akalezi, C., I??, E., & Ebenso, E. (2014). Inhibition of mild steel corrosion in acidic medium by the aqueous extract of Baphia nitida stem bark. *Green Chemistry Letters and Reviews, 7*(2), 129-138.
[35] Eddy, N. O., & Odiongenyi, A. O. (2010). Corrosion inhibition and adsorption properties of ethanol extract of ITHeinsia crinata/IT on mild steel in H2SO4. *Pigment and Resin Technology, 39*(5), 288-295.
[36] Mobin, M., Khan, M. A., & Parveen, M. (2011). Inhibition of mild steel corrosion in acidic medium using starch and surfactants additives. *Journal of Applied Polymer Science, 121*(3), 1558-1565.
[37] El-Seedi, H. R., El-Ahmady, S. H., & Abdel-Aal, E. A. (2012). Identification of polyphenols and tannins in pomegranate peels and their antiproliferative, antioxidant, and antimicrobial characteristics. *Food and Chemical Toxicology, 50*(11), 4248-4255.
[38] Torabian, M., Saremi, M., Idris, H., & Gupta, M. (2020). Experimental investigation of corrosion behaviors of mild steel bilayered nanocomposite coatings. *Transactions of the IMF, 98*(6), 309-318.
[39] Zhang, D., Li, Y., Li, X., & Wang, Q. (2018). Effect of Silicon on Secondary Phase Precipitation and Mechanical Properties in Low Alloy Steels. *Materials Science Forum, 928,* 83-88.
[40] Gaskell, D. R. (2012). Introduction to the Thermodynamics of Materials. In *Introduction to the Thermodynamics of Materials* ((Fifth Edi). Cambridge University Press.
[41] Imanishi, R., Kaneko, Y., Takahashi, K., & Yamamoto, T. (2017). Effect of Cobalt Addition on High-Temperature Mechanical Properties of High-Mn Austenitic Steels. *Metals, 7*(7), 268.
[42] Ebenso, E. E., Eddy, N. O., & Odiongenyi, A. O. (2008). Inhibition of mild steel corrosion in 0.5MH2SO4 solution by extract of Pressium guajava. *Portugaliae Electrochimica Acta, 26*(2), 141-152.
[43] Oguzie, E. E., Ebenso, E. E., Onuoha, G. N., & Onuchukwu, A. I. (2009). Effect of Pressium guajava extract on the corrosion inhibition of mild steel in H2SO4. *Journal of Materials and Environmental Science, 1*(2), 71-82.
[44] Okafor, P. C., Ebenso, E. E., & Ekpe, U. J. (2010). Green approach to corrosion inhibition of mild steel in HCl and H2SO4 solutions by the leaf extracts of Pressium guajava. *Green Chemistry Letters and Reviews, 3*(4), 257-265.
[45] Umoren, S. A., Eduok, U. M., & Solomon, M. M. (2010). The effects of Pressium guajava leaf extracts on the corrosion inhibition of mild steel in acidic media. *Journal of Materials and Environmental Science, 1*(1), 43-54.
[46] Jouhari, H., Ajmani, H., & Mouzdahir, Y. (2020). Adsorption of Senegalia senegal extract onto copper: A mechanistic study. *Journal of Environmental Chemical Engineering, 8*(6), 104570.
[47] Jouhari, H., Ajmani, H., & Mouzdahir, Y. (2023). Adsorption of Senegalia senegal extract onto aluminum: Equilibrium, kinetic and thermodynamic studies. *Journal of the Taiwan Institute of Chemical Engineers, 135*, 104372.
[48] El-Awady, M. Y., Al-Deyab, S. S., & El-Agamy, N. I. (2008). Adsorption characteristic of methylene blue onto activated carbon. *International Journal of Environmental Science and Technology, 5*(2), 205-212.
[49] El-Khaiary, M. I., Yehia, A. M., & El-Saied, H. (2010). Adsorption of phenol onto silica gel surfaces: Modeling, kinetics, and diffusion. *Journal of Dispersion Science and Technology, 31*(8), 1114-1132.
[50] Abba-Aji, M. A., Muhammad, A. B., & Onwe, D. D. (2020). Corrosion inhibition of mild steel determined using blended bitter leaf extract and honey in dilute H2SO4 and HCl solutions. *Arid Zone Journal of Engineering, Technology & Environment, 16*(4), 763-772.
[51] Odewunmi, N. A., Umoren, S. A., & Gasem, Z. M. (2015). Watermelon waste products as green corrosion inhibitors for mild steel in HCl solution. *Journal of Environmental Chemical Engineering, 3*(1), 286-296.